Higgs bosons near 125 GeV in the NMSSM with constraints at the GUT scale

Ulrich Ellwanger, Cyril Hugonie

Hindawi Publishing Corporation
Advances in High Energy Physics
Volume 2012, Article ID 625389, 18 pages
doi:10.1155/2012/625389

Research Article

Higgs Bosons Near 125 GeV in the NMSSM with Constraints at the GUT Scale

Ulrich Ellwanger[1] and Cyril Hugonie[2]

[1] *LPT, UMR 8627 CNRS, Université de Paris-Sud, 91405 Orsay, France*
[2] *LUPM, UMR 5299 CNRS, Université de Montpellier II, 34095 Montpellier, France*

Correspondence should be addressed to Ulrich Ellwanger, ellwanger@th.u-psud.fr

Received 21 May 2012; Accepted 3 July 2012

Academic Editor: Jun-jie Cao

We study the NMSSM with universal Susy breaking terms (besides the Higgs sector) at the GUT scale. Within this constrained parameter space, it is not difficult to find a Higgs boson with a mass of about 125 GeV and an enhanced cross-section in the diphoton channel. An additional lighter Higgs boson with reduced couplings and a mass $\lesssim 123$ GeV is potentially observable at the LHC. The NMSSM-specific Yukawa couplings λ and κ are relatively large and $\tan\beta$ is small, such that λ, κ, and the top Yukawa coupling are of $\mathcal{O}(1)$ at the GUT scale. The lightest stop can be as light as 105 GeV, and the fine-tuning is modest. WMAP constraints can be satisfied by a dominantly Higgsino-like LSP with substantial bino, wino, and singlino admixtures and a mass of ~60–90 GeV, which would potentially be detectable by XENON100.

1. Introduction

Recently, the ATLAS [1–3] and CMS [4–6] collaborations have presented evidence for a Higgs boson with a mass near 126 GeV (ATLAS) and 125 GeV (CMS in [6]). Interestingly, the best fit to the signal strength $\sigma^{\gamma\gamma} \equiv \sigma_{\rm prod}(H) \times BR(H \to \gamma\gamma)$ in the $\gamma\gamma$ search channel is about one standard deviation larger than expected in the Standard Model (SM), $\sigma^{\gamma\gamma}_{\rm obs}/\sigma^{\gamma\gamma}_{\rm SM} \sim 2$ for ATLAS [1, 2], and $\sigma^{\gamma\gamma}_{\rm obs}/\sigma^{\gamma\gamma}_{\rm SM} \sim 1.6$ for CMS [6].

Since then, several publications have studied the impact of a Higgs boson in the 125 GeV range on the parameter space of supersymmetric (Susy) extensions of the SM [7–38]. Whereas a Higgs boson in the 125 GeV range is possible within the parameter space of the Minimal Susy SM (MSSM) [7–13, 15, 17–21, 25, 29–37], large radiative corrections involving heavy stops are required, which aggravate the "little fine-tuning problem" of the MSSM. In addition, it would be difficult to explain a large enhancement of the diphoton signal strength in the MSSM [15, 34, 37].

Within the Next-to-Minimal Supersymmetric SM (NMSSM [39, 40]), a Higgs boson in the 125 GeV range is much more natural [7, 16, 21, 26, 27, 34]. Additional tree-level contributions and large singlet-doublet mixings in the CP-even Higgs sector can push up the mass of the mostly SM-like Higgs boson and, simultaneously, reduce its coupling to b-quarks which results in a substantial enhancement of its branching fraction into two photons [7, 16, 26, 34]. Studies of the parameter space of the general NMSSM—including the dark matter relic density and dark matter nucleon cross section—were performed in [34, 38].

An important question is whether these interesting features of the NMSSM survive universality constraints on the soft Susy breaking parameters at the GUT scale. Since this approach imposes severe restrictions on the sparticle masses and couplings, it allows to study whether these would be consistent with present constraints from direct and indirect sparticle searches, the dark matter relic density and dark matter direct detection experiments. Moreover, it allows to make predictions for future searches, both in the sparticle and the Higgs sector.

The (fully constrained) CNMSSM [41, 42] was analysed in [11] with the result that once a relic density in agreement with WMAP [43] is imposed, the Higgs boson mass can barely be above 123 GeV. We find that one should allow for deviations from full universality in the Higgs sector, both for the NMSSM-specific soft Susy breaking terms and the MSSM-like Higgs soft masses like in the MSSM studies in [8, 11, 17, 20]. In analogy to the NUHM version of the MSSM, we will refer to such a model as NUH-NMSSM for nonuniversal Higgs NMSSM. A first study of the NUH-NMSSM was made in [23] which was confined, however, to the more MSSM-like region of the parameter space of the NMSSM involving small values of the NMSSM-specific coupling λ and hence small NMSSM-specific effects in the CP-even Higgs sector.

In the present paper we study the NUH-NMSSM for large values of the NMSSM-specific coupling λ (and low $\tan\beta$), where the singlet-doublet mixing in the CP-even Higgs sector is large, and we find that the interesting features of the Higgs sector of the NMSSM observed in [7, 16, 21, 26, 27, 34] can remain present, including constraints from searches for squarks and gluinos from ATLAS and CMS [44–46], constraints on the dark matter relic density from WMAP [43] and on the dark matter nucleon cross section from XENON100 [47].

Our results in the Higgs sector originate essentially from the strong mixing between all three CP-even Higgs states in the NMSSM: first, a Higgs boson with a mass in the 125 GeV range can have an enhanced diphoton signal strength up to $\sigma^{\gamma\gamma}_{\text{obs}}/\sigma^{\gamma\gamma}_{\text{SM}} \sim 2.8$. Second, a lighter less SM-like Higgs boson H_1 exists, with small couplings to electroweak gauge bosons if $M_{H_1} \lesssim 114\,\text{GeV}$ (complying with LEP constraints [48]), but a possibly detectable production cross section at the LHC if $M_{H_1} \gtrsim 114\,\text{GeV}$. In fact, a strongly enhanced diphoton signal strength $\gtrsim 2$ of the Higgs boson H_2 with its mass in the 125 GeV range is possible only if $M_{H_1} \gtrsim 90\,\text{GeV}$. The heaviest CP-even Higgs boson H_3, like the heaviest MSSM-like CP-odd and charged Higgs bosons, has masses in the 250–650 GeV range, while the lightest mostly singlet-like CP-odd Higgs state has a mass in the 160–400 GeV range. These comply with constraints both from B-physics and direct Susy Higgs searches also for lower masses due to the low values of $\tan\beta$ considered here and the large singlet component of the lightest CP-odd state.

In the sparticle sector we require masses for the gluino and the first generation squarks to comply with constraints from present direct searches [44–46], but we also study the effect of a reduced sensitivity due to the more complicated decay cascades in the NMSSM [49]. The lightest stop $\widetilde{t}_1$ can be as light as ~105 GeV (still satisfying constraints from ATLAS [50] and the Tevatron [51], the latter due to its dominant decay into a chargino and a b-quark),

and the required fine-tuning among the parameters at the GUT scale remains modest. In the neutralino sector, the mixings among the five states (bino, wino, two Higgsinos, and the singlino) are large. The LSP, with a dominant Higgsino component and a mass of 60–90 GeV, has a relic density complying with the WMAP constraints [43] and a direct detection cross-section possibly within the reach of XENON100 [47]. However, the supersymmetric contribution to the anomalous magnetic moment of the muon is somewhat smaller than desired to account for the deviation of the measurement [52] from the SM.

In the next section we present the analysed parameter space of the NMSSM with boundary conditions at the GUT scale and the imposed phenomenological constraints; our results are given in Section 3 and conclusions in Section 4.

2. The NMSSM with Constraints at the GUT Scale

The NMSSM differs from the MSSM due to the presence of the gauge singlet superfield S. In the simplest Z_3 invariant realisation of the NMSSM, the Higgs mass term $\mu H_u H_d$ in the superpotential W_{MSSM} of the MSSM is replaced by the coupling λ of S to H_u and H_d and a self-coupling κS^3. Hence, in this simplest version the superpotential W_{NMSSM} is scale invariant and given by

$$W_{\text{NMSSM}} = \lambda \widehat{S}\widehat{H}_u \cdot \widehat{H}_d + \frac{\kappa}{3}\widehat{S}^3 + \cdots, \tag{2.1}$$

where hatted letters denote superfields, and the ellipsis denote the MSSM-like Yukawa couplings of $\widehat{H}_u$ and $\widehat{H}_d$ to the quark and lepton superfields. Once the real scalar component of $\widehat{S}$ develops a vev s, the first term in W_{NMSSM} generates an effective μ-term,

$$\mu_{\text{eff}} = \lambda s. \tag{2.2}$$

The soft Susy breaking terms consist of mass terms for the Higgs bosons H_u, H_d, S, squarks $\widetilde{q}_i \equiv (\widetilde{u}_{i_L}, \widetilde{d}_{i_L})$, $\widetilde{u}_{i_R}^c$, $\widetilde{d}_{i_R}^c$, and sleptons $\widetilde{\ell}_i \equiv (\widetilde{\nu}_{i_L}, \widetilde{e}_{i_L})$ and $\widetilde{e}_{i_R}^c$ (where $i = 1, \ldots, 3$ is a generation index):

$$\begin{aligned} -\mathcal{L}_0 = {} & m_{H_u}^2 |H_u|^2 + m_{H_d}^2 |H_d|^2 + m_S^2 |S|^2 + m_{\widetilde{q}_i}^2 \left|\widetilde{q}_i\right|^2 + m_{\widetilde{u}_i}^2 \left|\widetilde{u}_{i_R}^c\right|^2 + m_{\widetilde{d}_i}^2 \left|\widetilde{d}_{i_R}^c\right|^2 \\ & + m_{\widetilde{\ell}_i}^2 \left|\widetilde{\ell}_i\right|^2 + m_{\widetilde{e}_i}^2 \left|\widetilde{e}_{i_R}^c\right|^2, \end{aligned} \tag{2.3}$$

trilinear interactions involving the third generation squarks, sleptons, and the Higgs fields (neglecting the Yukawa couplings of the two first generations):

$$\begin{aligned} -\mathcal{L}_3 = {} & \Big(h_t A_t Q \cdot H_u \widetilde{u}_{3_R}^c + h_b A_b H_d \cdot Q \widetilde{d}_{3_R}^c + h_\tau A_\tau H_d \cdot L \widetilde{e}_{3_R}^c \\ & + \lambda A_\lambda H_u \cdot H_d S + \frac{1}{3}\kappa A_\kappa S^3 \Big) + \text{ h.c.}, \end{aligned} \tag{2.4}$$

and mass terms for the gauginos $\widetilde{B}$ (bino), $\widetilde{W}^a$ (winos), and $\widetilde{G}^a$ (gluinos):

$$-\mathcal{L}_{1/2} = \frac{1}{2}\left[M_1\widetilde{B}\widetilde{B} + M_2\sum_{a=1}^{3}\widetilde{W}^a\widetilde{W}_a + M_3\sum_{a=1}^{8}\widetilde{G}^a\widetilde{G}_a\right] + \text{h.c.} \tag{2.5}$$

Expressions for the mass matrices of the physical CP-even and CP-odd Higgs states—after H_u, H_d, and S have assumed vevs v_u, v_d, and s and including the dominant radiative corrections—can be found in [40] and will not be repeated here. The couplings of the CP-even Higgs states depend on their decompositions into the weak eigenstates H_d, H_u, and S, which are denoted by

$$\begin{aligned} H_1 &= S_{1,d}H_d + S_{1,u}H_u + S_{1,s}S, \\ H_2 &= S_{2,d}H_d + S_{2,u}H_u + S_{2,s}S, \\ H_3 &= S_{3,d}H_d + S_{3,u}H_u + S_{3,s}S. \end{aligned} \tag{2.6}$$

Then the reduced tree-level couplings (relative to a SM-like Higgs boson) of H_i to b quarks, τ leptons, t quarks, and electroweak gauge bosons V are

$$\begin{gathered} \frac{g_{H_ibb}}{g_{H_{\text{SM}}bb}} = \frac{g_{H_i\tau\tau}}{g_{H_{\text{SM}}\tau\tau}} = \frac{S_{i,d}}{\cos\beta}, \qquad \frac{g_{H_itt}}{g_{H_{\text{SM}}tt}} = \frac{S_{i,u}}{\sin\beta}, \\ \overline{g}_i \equiv \frac{g_{H_iVV}}{g_{H_{\text{SM}}VV}} = \cos\beta S_{i,d} + \sin\beta S_{i,u}. \end{gathered} \tag{2.7}$$

Mixings between the SU(2)-doublet and singlet sectors are always proportional to λ.

As compared to two independent parameters in the Higgs sector of the MSSM at tree level (often chosen as $\tan\beta$ and M_A), the Higgs sector of the NMSSM is described by the six parameters,

$$\lambda, \kappa, A_\lambda, A_\kappa, \tan\beta \equiv v_u/v_d, \mu_{\text{eff}}. \tag{2.8}$$

Then the soft Susy breaking mass terms for the Higgs bosons $m^2_{H_u}$, $m^2_{H_d}$, and m^2_S are determined implicitly by M_Z, $\tan\beta$, and μ_{eff}.

In constrained versions of the NMSSM (as in the constrained MSSM) one assumes that the soft Susy breaking terms involving gauginos, squarks, or sleptons are identical at the GUT scale:

$$\begin{gathered} M_1 = M_2 = M_3 \equiv M_{1/2}, \\ m^2_{\widetilde{q}_i} = m^2_{\widetilde{u}_i} = m^2_{\widetilde{d}_i} = m^2_{\widetilde{\ell}_i} = m^2_{\widetilde{e}_i} \equiv m^2_0, \\ A_t = A_b = A_\tau \equiv A_0. \end{gathered} \tag{2.9}$$

In the NUH-NMSSM considered here one allows the Higgs sector to play a special role: the Higgs soft mass terms $m^2_{H_u}$, $m^2_{H_d}$, and m^2_S are allowed to differ from m^2_0 (and determined

implicitly as noted above), and the trilinear couplings A_λ, A_κ can differ from A_0. Hence, the complete parameter space is characterized by

$$\lambda, \kappa, \tan\beta, \mu_{\text{eff}}, A_\lambda, A_\kappa, A_0, M_{1/2}, m_0, \tag{2.10}$$

where the latter five parameters are taken at the GUT scale.

Subsequently we are interested in regions of the parameter space implying large doublet-singlet mixing in the Higgs sector, that is, large values of λ (and κ) and low values of $\tan\beta$, which lead naturally to a SM-like Higgs boson H_2 in the 125 GeV range [7, 16, 21, 26, 27, 34]. Requiring $124\,\text{GeV} < M_{H_2} < 127\,\text{GeV}$ and $\sigma^{\gamma\gamma}_{\text{obs}}(H_2)/\sigma^{\gamma\gamma}_{\text{SM}} > 1$, we find

$$\begin{aligned} 0.41 < \lambda < 0.69, \\ 0.21 < \kappa < 0.46, \\ 1.7 < \tan\beta < 6, \end{aligned} \tag{2.11}$$

with many points for $\tan\beta \lesssim 2.5$. It is intriguing that with these choices at the weak scale, one obtains $\lambda \sim \kappa \sim h_t \sim \mathcal{O}(1)$ for the running couplings at the GUT scale; hence, all 3 Yukawa couplings are close to (but still below) a Landau singularity.

We assume $\mu_{\text{eff}} > 0$. $A_\kappa \lesssim 0$ at the weak scale is required for positive CP-odd Higgs masses squared. We found that, as a consequence, the coupled RG equations imply essentially $A_0, A_\lambda, A_\kappa < 0$ at the GUT scale. Constraints on the soft Susy breaking parameters depend strongly on the sparticle decay cascades. Using the absence of signal at the LHC in the jets and missing transverse momentum search channels, bounds in the m_0, $M_{1/2}$ plane have been derived in the CMSSM with $\tan\beta = 10$ [44–46]. In the NUH-NMSSM, however, we find lighter stops (due to the lower values of $\tan\beta$ implying a larger value of the top Yukawa coupling, which affects the RGE running of the soft Susy breaking stop masses) and a modified neutralino sector which reduces the sensitivity in these search channels [49].

Hence, to start with, we impose only constraints from sparticle searches at LEP [53] and the Tevatron [54, 55], and from stop searches at the Tevatron [51] and the LHC [50]. These imply

$$\begin{aligned} m_0 &\gtrsim 140\,\text{GeV}, \qquad M_{1/2} \gtrsim 270\,\text{GeV}, \\ m_{\tilde{q}} &\gtrsim 580\,\text{GeV}, \qquad M_{\tilde{g}} \gtrsim 640\,\text{GeV}. \end{aligned} \tag{2.12}$$

In addition we require that the fine-tuning Δ defined in (3.4) satisfies $\Delta < 120$, which implies upper bounds which will be discussed below. However, it is possible that the stronger CMSSM-like constraints in the $m_0, M_{1/2}$ plane [46] also apply to the NUH-NMSSM considered here. These stronger constraints further reduce the allowed points in the parameter space approximately to

$$m_{\tilde{q}} \gtrsim 1250\,\text{GeV}, \qquad M_{\tilde{g}} \gtrsim 850\,\text{GeV}, \tag{2.13}$$

but we implemented the constraints from [46] in the m_0, $M_{1/2}$ plane exactly. These constraints are used for the points shown in the Figures 1–3 below, but the difference between the

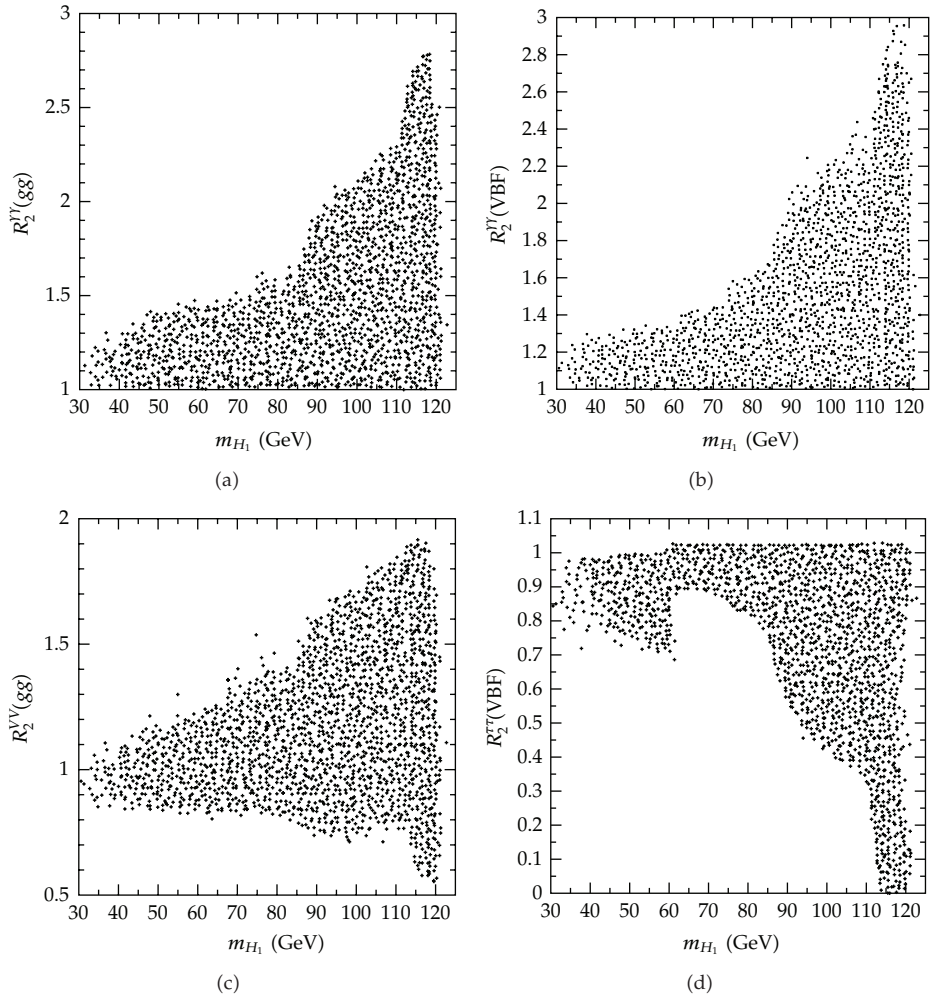

Figure 1: Reduced signal cross sections R_2 for H_2 with a mass in the 124–127 GeV range, as a function of M_{H_1} for a representative sample of viable points in parameter space. (a) $R_2^{\gamma\gamma}(gg)$ (diphoton channel, H_2 production via gluon fusion), (b) $R_2^{\gamma\gamma}$ (VBF) (diphoton channel, H_2 production via VBF), (c) R_2^{VV} (ZZ, WW channels, H_2 production via gluon fusion), and (d) $R_2^{\tau\tau}$ (VBF) ($\tau\tau$ channel, H_2 production via VBF).

constraints (2.12) and (2.13) has practically no impact on our results in the Higgs sector. Remarkably, regardless of the constraints in the m_0, $M_{1/2}$ plane, the lightest stop mass can be as low as ~105 GeV.

Together with these bounds on m_0, $M_{1/2}$, the above constraints on the Higgs sector and the LEP bound on the chargino mass lead to

$$\begin{aligned} 105 < \mu_{\text{eff}} < 205\,\text{GeV for weak constraints (2.12)},\\ 105 < \mu_{\text{eff}} < 160\,\text{GeV for strong constraints (2.13)}. \end{aligned} \tag{2.14}$$

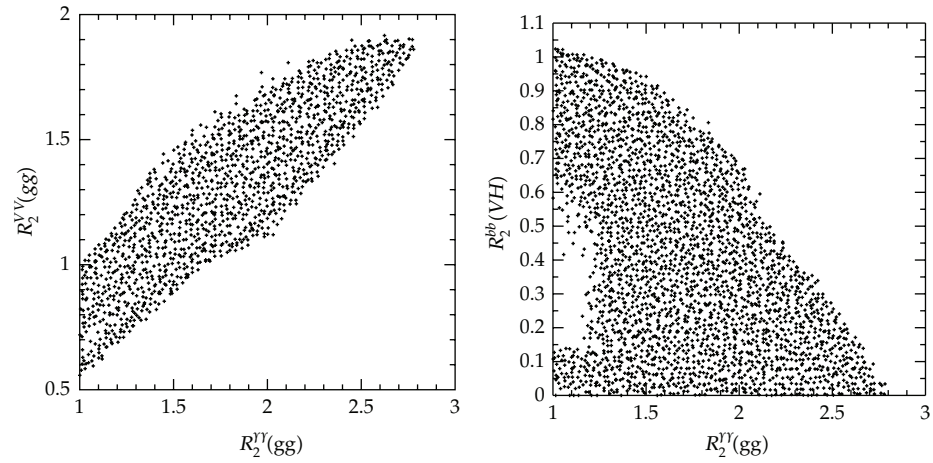

Figure 2: (a) $R_2^{VV}(gg)$ as function of $R_2^{\gamma\gamma}(gg)$. (b) $R_2^{b\bar{b}}(VH)$ (associate production $W/Z+H_2$ with $H_2 \to b\bar{b}$) as a function of $R_2^{\gamma\gamma}(gg)$.

Appropriate combinations of the bino/wino/higgsino/singlino components of χ_1^0 are required in order to satisfy the WMAP and XENON100 bounds. This leads to constraints on μ_{eff}—relevant for the higgsino components—as function of $M_{\tilde{g}}$, which is proportional to the bino/wino mass terms.

We have scanned the parameter space of the NUH-NMSSM given in (2.10) using a Markov Chain Monte Carlo (MCMC) technique, which yields a very large number of points (~10^6) satisfying all the phenomenological constraints described below. To do so, we have modified the code NMSPEC [56] inside NMSSMTools [57, 58] in order to allow for κ and μ_{eff} to be used as input parameters at the weak scale and to compute the Higgs soft masses $m_{H_u}^2$, $m_{H_d}^2$ at the GUT scale; a corresponding version 3.2.0 will be made public soon. In NMSPEC, the two-loop renormalization group equations (RGEs) between the weak and GUT scales are integrated numerically for all parameters. In the presence of boundary conditions both at the weak and the GUT scales as it is the case here, these can be satisfied only through an iterative process. This iterative process is not guaranteed to converge, notably for large Yukawa couplings as in (2.11). In fact, the RGE integration algorithm within the latest public version 3.1.0 of NMSSMTools had to be modified in version 3.2.0 to achieve convergence for large Yukawa couplings.

In the Higgs sector we have used two-loop radiative corrections from [59], and for the top quark pole mass we use $m_{\text{top}} = 172.9\,\text{GeV}$. Our results in the next section use the reduced Higgs production rates (normalized with respect to the SM production rates) in various channels. For gluon-gluon fusion we use the reduced Higgs-gluon coupling as computed in NMSSMTools, which takes care of all colored (s)particles in the loop. For the low values of $\tan\beta$ considered here, the top quark loop dominates by far and leads essentially to $g_{H_i tt}/g_{H_{\text{SM}}tt}$ as given in (2.7). Since a single particle loop dominates, radiative corrections not considered in NMSSMTools tend to cancel in the ratio to the SM. Likewise, Higgs production rates via associate production with W/Z ($\equiv V$) or vector boson fusion (VBF) are simply proportional to the SM rates rescaled by $\overline{g}_i^2$ defined in (2.7). The Higgs branching fractions are computed in NMSSMTools to the same accuracy both for the NMSSM and a SM-like Higgs boson, such

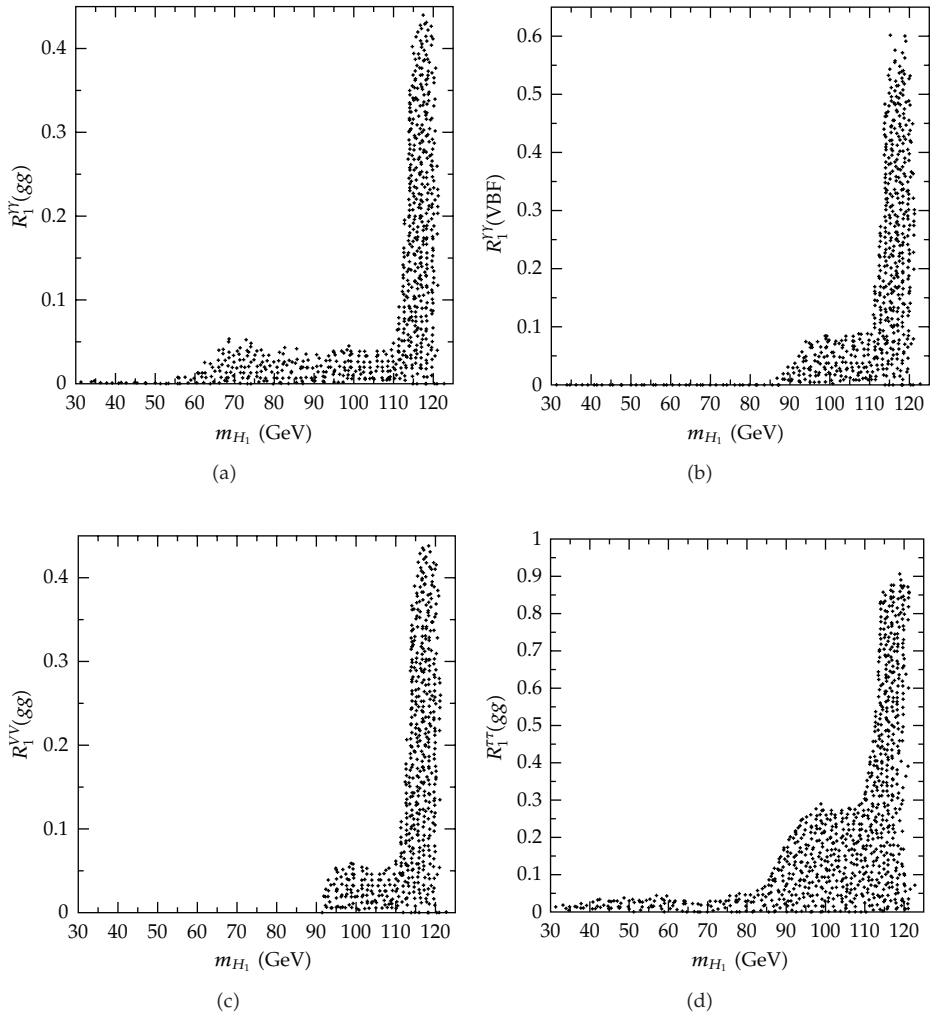

Figure 3: Reduced signal cross sections R_1 as a function of M_{H_1}. (a) $R_1^{\gamma\gamma}(gg)$ (diphoton channel, H_1 production via gluon fusion), (b) $R_1^{\gamma\gamma}$ (VBF) (diphoton channel, H_1 production via VBF), (c) $R_1^{VV}(gg)$ (ZZ and WW channels, H_1 production via gluon fusion), and (d) $R_1^{\tau\tau}$ (VBF) ($\tau\tau$ channel, H_1 production via VBF).

that radiative corrections not considered in NMSSMTools tend again to cancel in the ratio to the SM.

Next we turn to the imposed phenomenological constraints. In the Higgs sector we impose constraints from LEP [48], which still allow for a Higgs mass below 114 GeV if its coupling to the Z boson is reduced. Constraints on Higgs bosons from the LHC are those implemented in version 3.1.0 of NMSSMTools, which are based on public ATLAS and CMS results available at the end of 2011, including constraints from CMS on heavy MSSM-like Higgs bosons decaying to tau pairs [60]. In version 3.2.0, however, we have updated the important $\gamma\gamma$ search channel with the results from ATLAS [2] and CMS [5]. In order to fit the evidence of both experiments in the $\gamma\gamma$ channel, we impose $124\,\text{GeV} < M_H < 127\,\text{GeV}$, which is satisfied exclusively by H_2 for larger values of λ, and we require a good visibility of

H_2 in the $\gamma\gamma$ channel, that is, $\sigma^{\gamma\gamma}_{\rm obs}(H_2)/\sigma^{\gamma\gamma}_{\rm SM} > 1$ in both the gluon fusion and VBF production modes.

Also the constraints from B-physics are those implemented in version 3.1.0 of NMSSMTools. In spite of charged (resp., CP-odd) Higgs masses as low as ~250 (resp., 160) GeV, these are easily satisfied for low values of $\tan\beta$ or a large singlet component for the lightest CP-odd state (i.e., the couplings of these Higgs bosons to b-quarks are hardly enhanced with respect to the SM Higgs).

The dark matter relic density and direct detection cross section of the LSP χ^0_1 (the lightest neutralino) are computed with the help of MicrOmegas [61–63] implemented in NMSSMTools. The default constraints $0.094 < \Omega h^2 < 0.136$ are slightly weaker than the most recent ones from WMAP [43], but this has no impact on the viable regions in parameter space (only on the number of points retained). We also apply the bounds from XENON100 [47] on the spin-independent χ^0_1-nucleon cross section (roughly $\sigma^{si}(p) \lesssim 10^{-8}$ pb for $M_{\chi^0_1} \sim$ 60–90 GeV).

Since we hardly find light sleptons of the second generation (and again due to the low values of $\tan\beta$), the Susy contribution Δa_μ to the anomalous magnetic moment of the muon is below $\Delta a_\mu \lesssim 7 \cdot 10^{-10}$, violating the constraint implemented in NMSSMTools. However, it still improves the discrepancy between the SM and the measured value [52] and can reduce the discrepancy to two standard deviations depending on the employed SM value.

3. Results

Some remarks on our results have already been made above. Notably we have no difficulties to find points in the parameter space satisfying the above constraints, including the dark matter relic density and the direct detection cross section, $124\,\text{GeV} < M_{H_2} < 127\,\text{GeV}$ and $R^{\gamma\gamma}_2 > 1$, where we define

$$R^{\gamma\gamma}_2 \equiv \frac{\sigma^{\gamma\gamma}_{\rm obs}(H_2)}{\sigma^{\gamma\gamma}_{\rm SM}}. \tag{3.1}$$

The mechanism behind this enhancement has been discussed earlier in [7, 16, 64]: the $BR(H_2 \to \gamma\gamma)$ is strongly enhanced due to a reduced total width (dominated by $\Gamma(H_2 \to b\bar{b})$) for a small reduced coupling $g_{H_2bb}/g_{H_{\rm SM}bb}$ in (2.7), that is, a small value of the mixing angle $S_{2,d}$, in spite of a milder reduction of the partial width $\Gamma(H_2 \to \gamma\gamma)$. This occurs for large singlet-doublet mixing (which also leads to an increase of M_{H_2}) and requires that the third eigenstate H_3 is not decoupled, that is, not too heavy. The enhancement of the $BR(H_2 \to \gamma\gamma)$ also overcompensates a milder reduction of the production cross section of H_2 due to singlet-doublet mixing.

The reduction of the total width leads also to a potential increase of the reduced signal rate in the ZZ/WW channels (via gluon fusion),

$$R^{VV}_2(gg) \equiv \frac{\sigma^{ZZ}_{\rm obs}(gg \to H_2)}{\sigma^{ZZ}_{\rm SM}(gg \to H)} = \frac{\sigma^{WW}_{\rm obs}(gg \to H_2)}{\sigma^{WW}_{\rm SM}(gg \to H)}, \tag{3.2}$$

in spite of the reduction of the partial widths $\Gamma(H_2 \to ZZ/WW)$ due to singlet-doublet mixing. A fourth interesting reduced signal cross section is the $\tau\tau$ channel via VBF:

$$R_2^{\tau\tau}(\text{VBF}) \equiv \frac{\sigma_{\text{obs}}^{\tau\tau}(WW \to H_2)}{\sigma_{\text{SM}}^{\tau\tau}(WW \to H)}, \tag{3.3}$$

which tends to be reduced, however, for a small mixing angle $S_{2,d}$.

Singlet-doublet mixing angles are typically large, if the eigenstates are close in mass. Hence, we should expect that $R_2^{\gamma\gamma}$ is the larger, the closer M_{H_1} is to M_{H_2}, that is, the heavier is H_1. Subsequently we consider separately $R_2^{\gamma\gamma}(gg)$ (where H_2 is produced via gluon fusion) and $R_2^{\gamma\gamma}(\text{VBF})$ (where H_2 is produced via VBF). In Figure 1 we show $R_2^{\gamma\gamma}(gg)$, $R_2^{\gamma\gamma}(\text{VBF})$, $R_2^{VV}(gg)$, and $R_2^{\tau\tau}(\text{VBF})$ as a function of M_{H_1} for a representative sample of ~2000 points in the scanned parameter space of the semiconstrained NMSSM described above. All points satisfy the WMAP bound on the dark matter relic density, the XENON100 bound on $\sigma^{si}(p)$, and the stronger lower bound on $M_{1/2}$ given in (2.13). Relaxing this bound to the one given in (2.12) does not lead to additional regions in Figure 1.

We see that, as expected, the ratios $R_2^{\gamma\gamma}(gg)$, $R_2^{\gamma\gamma}(\text{VBF})$, and $R_2^{VV}(gg)$ can increase with M_{H_1}, and $R_2^{\gamma\gamma}(gg)$ can become as large as 2.8 for $M_{H_1} \gtrsim 115\,\text{GeV}$. The inverse conclusion does not hold: $M_{H_1} \gtrsim 115$ GeV does not imply $R_2^{\gamma\gamma} > 2$. $R_2^{\tau\tau}(\text{VBF})$ is below ~1, and the very small values of $R_2^{\tau\tau}(\text{VBF})$ correspond to the highest values of $R_2^{\gamma\gamma}(gg)$. The jump in $R_2^{\tau\tau}(\text{VBF})$ near $M_{H_1} \sim 60\,\text{GeV}$ is caused by a combination of LEP, B-physics, and WMAP constraints as well as the condition $R_2^{\gamma\gamma} > 1$. For M_{H_2} in the range 124–127 GeV, none of these reduced signal rates show a significant dependency on M_{H_2}; corresponding plots would only transcribe the LHC constraints on each rate as a function M_{H_2}, but they would not provide additional informations and are hence omitted.

In Figure 1(c) we see that $R_2^{VV}(gg)$ may be below 1. In fact, the "best fit" to $R_2^{WW}(gg)$ by ATLAS [1] and by CMS [4] is below 1, whereas the "best fit" to $R_2^{ZZ}(gg)$ is below 1 by CMS [4], but above 1 by ATLAS [1]. We recall that we have $R_2^{WW}(gg) \equiv R_2^{ZZ}(gg) \equiv R_2^{VV}(gg)$. Hence, it may be interesting to see to which extend $R_2^{VV}(gg)$ and $R_2^{\gamma\gamma}(gg)$ ($\sim R_2^{\gamma\gamma}(\text{VBF})$) are correlated. This correlation is shown in Figure 2(a), and we see that $R_2^{VV}(gg) < 1$ is possible for $R_2^{\gamma\gamma}(gg)$ up to ~1.5.

Recently, excesses compatible with a Higgs boson in the 125 GeV range have also been observed at the Tevatron [65]. Here, the dominant excess originates from associated VH production with $H \to b\bar{b}$. The corresponding reduced signal rate for the candidate H_2, $R_2^{b\bar{b}}(VH)$ (which is equal to $R_2^{\tau\tau}(\text{VBF})$) cannot be very small given the observations at the Tevatron. In Figure 2(b) we show $R_2^{b\bar{b}}(VH)$ against $R_2^{\gamma\gamma}(gg)$. We see that $R_2^{b\bar{b}}(VH) \gtrsim 0.7$ is possible only for $R_2^{\gamma\gamma}(gg) \lesssim 2$, but $R_2^{\gamma\gamma}(gg) \gtrsim 1.6$ still allows for $R_2^{b\bar{b}}(VH) \gtrsim 0.9$.

Obviously the reduced signal rates of H_1 are also very important. For instance, H_1 could be compatible with the excess of events observed by CMS for $M_H \sim 119.5\,\text{GeV}$ in the ZZ channel [4]. On the other hand, for $M_H \sim 95$–$100\,\text{GeV}$ the upper bounds from LEP on its reduced coupling to the Z boson are particularly weak, and a mostly (but not completely) singlet-like H_1 could explain the mild excess of events observed there [48, 66, 67]. The corresponding reduced signal cross-sections as a function of M_{H_1} are shown in Figure 3. As explained in [16], the reduced signal cross-section in the $b\bar{b}$ channel at LEP coincides with $R^{\tau\tau}(\text{VBF})$.

We see that the reduced signal cross-sections are mostly small for $M_{H_1} \lesssim 110\,\text{GeV}$ where the singlet component of H_1 is large, but $R_1^{\tau\tau}(\text{VBF})$ can be as large as ~0.25 for

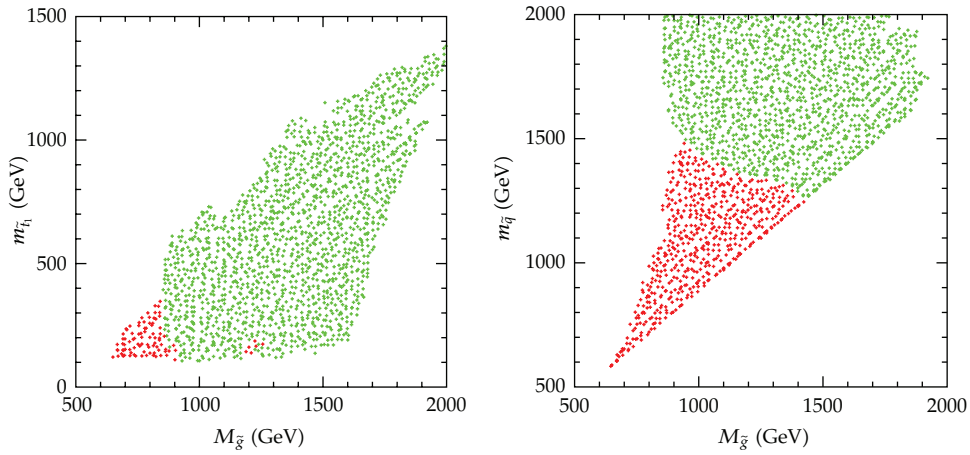

(a) (b)

Figure 4: $m_{\tilde{t}_1}$ (a) and $m_{\tilde{q}}$ (b) as a function of $M_{\tilde{g}}$. Points in red (darker points) satisfy the weaker bounds (2.12), but not the stronger bounds (2.13), while points in green (brighter) satisfy both constraints.

$M_{H_1} \sim$ 95–100 GeV which is interesting given the mild excess of events observed at LEP. On the other hand, for $M_{H_1} \gtrsim 110$ GeV, $R_1^{\gamma\gamma}(gg)$, $R_1^{\gamma\gamma}$(VBF) and $R_1^{VV}(gg)$ can become as large as ~0.5 and $R_1^{\tau\tau}$(VBF) as large as ~0.9, hence, H_1 is potentially detectable.

The Higgs sector of the NMSSM contains a third CP-even state H_3, two CP-odd states A_1 and A_2, and, as in the MSSM, a charged Higgs boson $H_\pm$. We find that the lightest CP-odd state A_1 is mostly singlet-like with a mass in the range 160–400 GeV, and hardly visible at the LHC due to its small production cross-sections. The states H_3, A_2, and $H_\pm$ all have similar masses in the 250–650 GeV range and would also be difficult to see at the LHC due to the small value of $\tan\beta$ in the region of the parameter space of interest (2.11).

The masses of the sparticles are essentially determined by $M_{1/2}$, m_0, A_0, and μ_{eff}. In Figure 4 we show the mass $m_{\tilde{q}}$ of the lightest first generation squark (d_R for our choice of parameters) as well as the mass $m_{\tilde{t}_1}$ of the lightest (mostly right-handed) stop as a function of the gluino mass $M_{\tilde{g}}$. Here it makes a difference whether we impose the weaker bounds (2.12) or the stronger bounds (2.13): points in red satisfy only the weaker bounds while points in green satisfy both constraints. For $M_{\tilde{g}} \gtrsim 640$ GeV, a stop mass as small as 105 GeV is not excluded by present searches at the LHC [50], but could become observable in the near future.

It is known that the stop mass has an impact on the fine-tuning with respect to the fundamental parameters of Susy extensions of the SM, due to its impact on the running soft Susy breaking Higgs mass terms. In addition, both are affected by the gluino mass. We have estimated the quantitative amount of fine-tuning with respect to the parameters at the GUT scale following the procedure outlined in [68]. There, a fine-tuning measure

$$\Delta = \text{Max}\left\{\Delta_i^{\text{GUT}}\right\}, \qquad \Delta_i^{\text{GUT}} = \left|\frac{\partial \ln(M_Z)}{\partial \ln\left(p_i^{\text{GUT}}\right)}\right|, \tag{3.4}$$

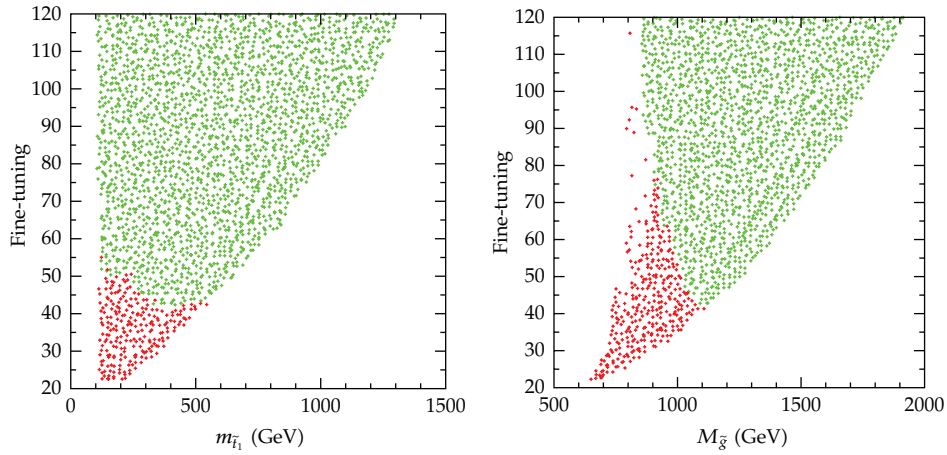

(a) (b)

Figure 5: Fine-tuning as a function of $m_{\tilde{t}_1}$ (a) and $M_{\tilde{g}}$ (b). The color code is as in Figure 4.

was used, where p_i^{GUT} are all parameters at the GUT scale (Yukawa couplings and soft Susy breaking terms). Note that sometimes $\ln(M_Z^2)$ instead of $\ln(M_Z)$ is used in the definition of Δ, leading to an obvious factor of 2. We find that Δ, shown as a function of $m_{\tilde{t}_1}$ and $M_{\tilde{g}}$ in Figure 5, is dominated as usual by $p_i^{\mathrm{GUT}} = M_{1/2}$.

We see that the fine-tuning $1/\Delta$ can be as low as $\mathcal{O}(5\%)$ (with the definition in (3.4)) in the range of smaller stop and gluino masses allowed by the weaker lower bounds (2.12), and still as low as $\mathcal{O}(2.5\%)$ in the range of stop and gluino masses allowed by the stronger bounds (2.13). Both values are an order of magnitude better than in the MSSM [69].

Turning to the neutralino sector we observe, as in the CP-even Higgs sector, large mixing angles involving all 5 neutralinos of the NMSSM. The lightest eigenstate χ_1^0 (the LSP) is mostly higgsino-like, but with sizeable bino, wino, and singlino components and a mass in the 60–90 GeV range. The lower bound on $M_{\chi_1^0}$ follows from the conditions that invisible decays $H_2 \to \chi_1^0\chi_1^0$ do not spoil the condition $\sigma^{\gamma\gamma}_{\mathrm{obs}}(H_2)/\sigma^{\gamma\gamma}_{\mathrm{SM}} > 1$, together with the lower LEP bound on chargino masses. Its direct detection cross-section is reduced with respect to pure higgsino-like neutralinos, and can well comply with the constraints from XENON100. In Figure 6 we show the spin-independent neutralino-proton scattering cross-section $\sigma^{si}(p)$ as a function of $M_{\chi_1^0}$. We see that the stronger bounds (2.13) imply $60\,\mathrm{GeV} \lesssim M_{\chi_1^0} \lesssim 85\,\mathrm{GeV}$, similar to the range within the general NMSSM obtained in [34]. In particular, the plateau observed in Figure 6 for $80 \lesssim M_{\chi_1^0} \lesssim 90\,\mathrm{GeV}$ and $\sigma^{si}(p) \sim 10^{-7}\,\mathrm{pb}$, corresponding to small values of $m_0, M_{1/2}$ and a mostly bino-like χ_1^0, is excluded by both the XENON100 and the strong LHC Susy constraints. The spin-independent neutralino-proton scattering cross-section $\sigma^{si}(p)$ can vary over a wide range both above and below the XENON100 limit [47] (which remains to be confirmed by other experiments), but plenty of points would satisfy this constraint and become observable in the future.

It may be interesting to know some of the properties of the Higgs and sparticle sectors beyond the ones shown in the scatter plots above; to this end we show two benchmark points in Table 1. The point (1) has $M_{H_1} \sim 100\,\mathrm{GeV}$, the point (2) $M_{H_1} \sim 120\,\mathrm{GeV}$, and they differ in

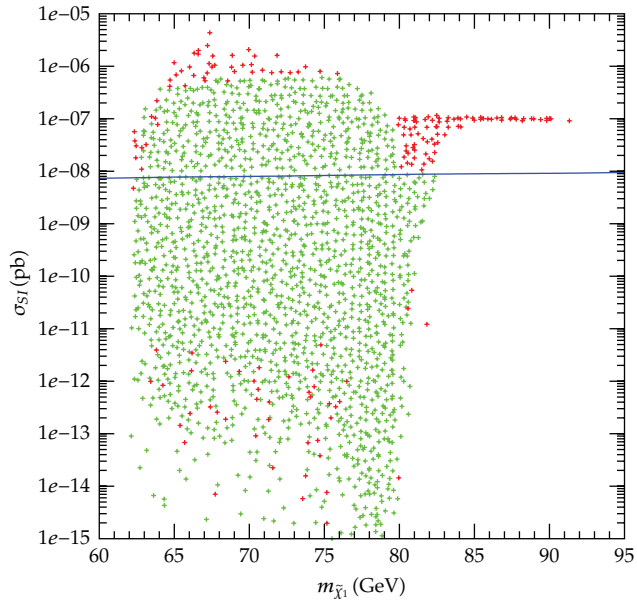

Figure 6: The spin-independent neutralino-proton scattering cross section $\sigma^{si}(p)$ as a function of $M_{\chi_1^0}$. The blue line indicates the bound from XENON100 [47], and we have added points violating this bound (but respecting all the others). The color code is as in Figure 4.

the values for $M_{1/2}$ and m_0. The branching fractions of $\tilde{t}_1$ are similar for both points: $BR(\tilde{t}_1 \to \chi_1^{\pm} + b) \sim 0.7$, $BR(\tilde{t}_1 \to \chi_1^0 + t) \sim 0.2$, $BR(\tilde{t}_1 \to \chi_2^0 + t) \sim 0.1$.

4. Conclusions

It has already been noted in [7, 16, 21, 26, 27, 34] that the NMSSM can naturally accomodate Higgs bosons in the 124–127 GeV mass range. In addition, the NMSSM can explain excesses in the $\gamma\gamma$ channel, as well as potential excesses at different values of the Higgs mass (due to the extended Higgs sector). In the present paper we have shown that these features persist in the constrained NMSSM with nonuniversal Higgs sector, designated here as NUH-NMSSM. The dominant deviation from full universality of all soft Susy breaking terms at the GUT scale originates from the need to have $m_{H_u} > m_0$.

The following properties of the Higgs sector are peculiar:

(i) the signal rate in the $\gamma\gamma$ channel can be 2.8 as large as the one of a SM-like Higgs boson, provided the mass of the lighter CP-even state H_1 is in the 115–123 GeV range;

(ii) requiring a visible signal rate in the $b\bar{b}$ channel of 0.9 times the SM value allows for a signal rate in the $\gamma\gamma$ channel about 1.6 as large as the one of a SM-like Higgs boson;

(iii) the lighter CP-even state H_1 could explain a mild excess of events around 95–100 GeV observed at LEP, or a second visible Higgs boson below ~123 GeV.

Table 1: Properties of two benchmark points corresponding to different values of M_{H_1}. All dimensionful parameters are given in GeV. The components of χ_1^0, as well as the components of H_i, are defined such that their squares sum up to 1. The Susy contributions Δa_μ to the muon anomalous magnetic moment are those given by NMSSMTools without any theoretical errors.

Point	(1)	(2)
Param. at $M_{\rm GUT}$:		
$M_{1/2}$	600	525
m_0	600	960
A_0	−1550	−1140
A_λ	−625	−575
A_κ	−275	−360
m_{H_u}	1670	1880
m_{H_d}	445	757
m_S	885	1380
λ	0.96	1.48
κ	0.73	1.08
h_t	0.83	0.97
Param. at $M_{\rm Susy}$:		
λ	0.545	0.6
κ	0.253	0.321
$\tan\beta$	2.40	2.29
$\mu_{\rm eff}$	120	122
Sparticle masses:		
$m_{\tilde{g}}$	1390	1250
$m_{\tilde{q}}$	1320	1400
$m_{\tilde{t}_1}$	359	463
$m_{\tilde{b}_1}$	1001	1060
$m_{\tilde{\tau}_1}$	528	900
$M_{\chi_1^\pm}$	108	108
$M_{\chi_1^0}$	77	78
Components of χ_1^0:		
$\widetilde{B}$	0.20	0.25
$\widetilde{W}$	−0.16	−0.20
$\widetilde{H}_d$	0.48	0.52
$\widetilde{H}_u$	−0.70	−0.70
$\widetilde{S}$	0.46	0.37
Ωh^2	0.10	0.10
$\sigma^{si}(p)$ $[10^{-8}\,\text{pb}]$	1.00	0.13
Δa_μ $[10^{-10}]$	0.93	0.52
M_{H_1}	100	120
Components of H_1:		
H_d	0.39	0.50
H_u	0.34	0.74
S	0.86	0.45
$R_1^{\gamma\gamma}(gg)$	0.01	0.32
$R_1^{\gamma\gamma}(\text{VBF})$	0.03	0.40
$R_1^{VV}(gg)$	0.03	0.34
$R_1^{\tau\tau}(\text{VBF})$	0.23	0.88
M_{H_2}	124	125

Table 1: Continued.

Point	(1)	(2)
Components of H_2:		
H_d	0.26	0.04
H_u	0.85	−0.54
S	−0.45	0.84
$R_2^{\gamma\gamma}(gg)$	1.54	1.77
$R_2^{\gamma\gamma}$(VBF)	1.42	0.98
$R_2^{VV}(gg)$	1.22	1.01
$R_2^{\tau\tau}$(VBF)	0.63	0.03
M_{H_3}	329	305
Components of H_3:		
H_d	0.88	0.86
H_u	−0.40	−0.40
S	−0.25	−0.30
$R_3^{\gamma\gamma}(gg)$	0.21	0.29
$R_3^{\gamma\gamma}$(VBF)	0.0006	0.0007
$R_3^{VV}(gg)$	0.001	0.002
$R_3^{\tau\tau}$(VBF)	0.04	0.03

In the sparticle sector, the assumption of universality at the GUT scale leads to the following features:

(i) the mass of the lightest stop can be as small as 105 GeV, complying with present constraints for $M_{\tilde{g}} \gtrsim 640\,\text{GeV}$;

(ii) the fine-tuning with respect to parameters at the GUT scale remains modest, an order of magnitude below the one required in the MSSM;

(iii) the eigenstates in the neutralino sector are strongly mixed, and the lightest neutralino can have a relic density in agreement with WMAP constraints. Its direct detection cross-section can be above or below present XENON100 bounds; most of the points below these bounds should be observable in the near future.

Given the large values of the NMSSM-specific coupling λ, all scenarios presented here differ strongly from the MSSM (also by the low value of $\tan\beta$). The fact that all 3 Yukawa couplings λ, κ, and h_t are of $\mathcal{O}(1)$ at the GUT scale may hint at some strong dynamics present at that scale. It is possible that the deviation from full universality of soft Susy breaking terms at the GUT scale remains confined to $m_{H_u} > m_0$; such possibilities require further studies.

Of course, first of all the present evidence for a Higgs boson in the 124–127 GeV mass range should be confirmed by more data; then possible evidence for non-SM properties of the Higgs sector like an enhanced cross-section in the diphoton channel will show whether the scenarios presented here are realistic.

Acknowledgments

U. Ellwanger acknowledges support from the French ANR LFV-CPV-LHC. C. Hugonie acknowledges support from the French ANRJ TPADMS.

References

[1] G. Aad et al., "Combined search for the Standard Model Higgs boson using up to 4.9 fb^{-1} of pp collision data at $\sqrt{s}$ = 7Tev with the ATLAS detector at the LHC," *Physics Letters B*, vol. 710, no. 1, pp. 49–66, 2012.

[2] [ATLAS Collaboration], "Search for the Standard Model Higgs boson in the diphoton decay channel with 4.9 fb^{-1} of pp collisions at $\sqrt{s}$ = 7Tev with ATLAS," *Physical Review Letters*, vol. 108, no. 11, Article ID 111803, 19 pages, 2012.

[3] G. Aad, B. Abbott, J. Abdallah et al., "An update to the combined search for the Standard Model Higgs boson with the ATLAS detector at the LHC using up to 4.9 fb^{-1} of pp collision data at $\sqrt{s}$ = 7Tev," *Physics Letters B*, vol. 710, no. 1, pp. 49–66, 2012.

[4] S. Chatrchyan, V. Khachatryan, A. M. Sirunyan, and A. Tumasyan, "Combined results of searches for the standard model Higgs boson in pp collisions at $\sqrt{s}$ = 7Tev," *Physics Letters B*, vol. 710, no. 1, pp. 26–48, 2012.

[5] S. Chatrchyan, V. Khachatryan, A. M. Sirunyan, and A. Tumasyan, "Search for the standard model Higgs boson decaying into two photons in pp collisions at $\sqrt{s}$ = 7Tev," *Physics Letters B*, vol. 710, no. 3, pp. 403–425, 2012.

[6] C. M. S. Collaboration, "A search using multivaraite techniques for a standard model Higgs boson decaying into two photons," CMS-PAS-HIG-12-001.

[7] L. J. Hall, D. Pinner, and J. T. Ruderman, "A natural SUSY higgs near 126 GeV," *Journal of High Energy Physics*, vol. 1204, p. 131, 2012.

[8] H. Baer, V. Barger, and A. Mustafayev, "Implications of a 125 GeV higgs scalar for LHC SUSY and neutralino dark matter searches," *Physical Review D*, vol. 85, Article ID 075010, 2012.

[9] J. L. Feng, K. T. Matchev, and D. Sanford, "Focus point supersymmetry redux," *Physical Review D*, vol. 85, no. 7, Article ID 075007, 2012.

[10] S. Heinemeyer, O. Stål, and G. Weiglein, "Interpreting the LHC Higgs search results in the MSSM," *Physics Letters B*, vol. 710, no. 1, pp. 201–206, 2012.

[11] A. Arbey, M. Battaglia, A. Djouadi, F. Mahmoudi, and J. Quevillon, "Implications of a 125 GeV Higgs for supersymmetric models," *Physics Letters B*, vol. 708, no. 1-2, pp. 162–169, 2012.

[12] A. Arbey, M. Battaglia, and F. Mahmoudi, "Constraints on the MSSM from the Higgs sector: A pMSSM study of Higgs searches, $B_s^0 \to \mu^+\mu^-$ and dark matter direct detection," *European Physical Journal C*, vol. 72, no. 3, pp. 1–13, 2012.

[13] P. Draper, P. Meade, M. Reece, and D. Shih, "Implications of a 125 GeV Higgs boson for the MSSM and low-scale supersymmetry breaking," *Physical Review D*, vol. 85, no. 9, Article ID 095007, 2012.

[14] T. Moroi, R. Sato, and T. T. Yanagida, "Extra matters decree the relatively heavy Higgs of mass about 125 GeV in the supersymmetric model," *Physics Letters B*, vol. 709, no. 3, pp. 218–221, 2012.

[15] M. Carena, S. Gori, N. R. Shah, and C. E. M. Wagner, "A 125 GeV SM-like Higgs in the MSSM and the $\gamma\gamma$ rate," *Journal of High Energy Physics*, vol. 2012, no. 3, article 014, 2012.

[16] U. Ellwanger, "A Higgs boson near 125 GeV with enhanced di-photon signal in the NMSSM," *Journal of High Energy Physics*, vol. 2012, no. 3, article 044, 2012.

[17] O. Buchmueller, R. Cavanaugh, A. de Roeck et al., "Higgs and supersymmetry," *European Physical Journal C*, vol. 72, no. 6, pp. 1–14, 2012.

[18] S. Akula, B. Altunkaynak, D. Feldman, P. Nath, and G. Peim, "Higgs boson mass predictions in SUGRA unification, recent LHC-7 results, and dark matter," *Physical Review D*, vol. 85, Article ID 075001, 2012.

[19] M. Kadastik, K. Kannike, A. Racioppi, and M. Raida, "Implications of the 125 GeV Higgs boson for scalar dark matter and for the CMSSM phenomenology," *Journal of High Energy Physics*, vol. 2012, no. 5, article 061, 2012.

[20] J. Cao, Z. Heng, D. Li, and J. M. Yang, "Current experimental constraints on the lightest Higgs boson mass in the constrained MSSM," *Physics Letters B*, vol. 710, no. 4-5, pp. 665–670, 2012.

[21] A. Arvanitaki and G. Villadoro, "A non standard model higgs at the LHC as a sign of naturalness," *Journal of High Energy Physics*, vol. 2012, no. 2, article 144, 2012.

[22] M. Gozdz, "Lightest Higgs boson masses in the R-parity violating supersymmetry," http://arxiv.org/abs/1201.0875.

[23] J. F. Gunion, Y. Jiang, and S. Kraml, "The constrained NMSSM and Higgs near 125 GeV," *Physics Letters B*, vol. 710, no. 3, pp. 454–459, 2012.

[24] P. Fileviez Pérez, "SUSY spectrum and the Higgs mass in the BLMSSM," *Physics Letters B*, vol. 711, no. 5, pp. 353–359, 2012.

[25] N. Karagiannakis, G. Lazarides, and C. Pallis, "Dark matter and higgs mass in the CMSSM with Yukawa Quasi-Unification," http://arxiv.org/abs/1201.2111.
[26] S. F. King, M. Mühlleitner, and R. Nevzorov, "NMSSM Higgs benchmarks near 125 GeV," *Nuclear Physics B*, vol. 860, no. 2, pp. 207–244, 2012.
[27] Z. Kang, J. Li, and T. Li, "On the Naturalness of the (N)MSSM," http://arxiv.org/abs/1201.5305.
[28] C.-F. Chang, K. Cheung, Y.-C. Lin, and T.-C. Yuan, "Mimicking the standard model Higgs boson in UMSSM," *Journal of High Energy Physics*, vol. 2012, no. 6, Article ID 51, 2012.
[29] L. Aparicio, D. G. Cerdeño, and L. E. Ibáñez, "A 119-125 GeV Higgs from a string derived slice of the CMSSM," *Journal of High Energy Physics*, vol. 2012, no. 4, Article ID 126, 2012.
[30] L. Roszkowski, E. M. Sessolo, and Y.-L. S. Tsai, "Bayesian implications of current LHC supersymmetry and dark matter detection searches for the constrained MSSM," http://arxiv.org/abs/1202.1503.
[31] J. Ellis and K. A. Olive, "Revisiting the Higgs mass and dark matter in the CMSSM," *European Physical Journal C*, vol. 72, no. 5, pp. 1–13, 2012.
[32] H. Baer, V. Barger, and A. Mustafayev, "Neutralino dark matter in mSUGRA/CMSSM with a 125 GeV light higgs scalar," *Journal of High Energy Physics*, vol. 2012, no. 5, Article ID 091, 2012.
[33] N. Desai, B. Mukhopadhyaya, and S. Niyogi, "Constraints on invisible Higgs decay in MSSM in the light of diphoton rates from the LHC," http://arxiv.org/abs/1202.5190.
[34] J. Cao, Z. Heng, J. M. Yang, Y. Zhang, and J. Zhu, "A SM-like Higgs near 125 GeV in low energy SUSY: a comparative study for MSSM and NMSSM," *Journal of High Energy Physics*, vol. 2012, no. 3, Article ID 086, 2012.
[35] L. Maiani, A. D. Polosa, and V. Riquer, "Probing minimal supersymmetry at the LHC with the Higgs boson masses," *New Journal of Physics*, vol. 14, Article ID 073029, 2012.
[36] T. Cheng, J. Li, T. Li, D. V. Nanopoulos, and C. Tong, "Electroweak supersymmetry around the electroweak scale," http://arxiv.org/abs/1202.6088 .
[37] N. Christensen, T. Han, and S. Su, "MSSM Higgs bosons at the LHC," *Physical Review D*, vol. 85, no. 11, Article ID 115018, 2012.
[38] D. A. Vasquez, G. Belanger, C. Boehm, J. Da Silva, P. Richardson, and C. Wymant, "The 125 GeV Higgs in the NMSSM in light of LHC results and astrophysics constraints," http://arxiv.org/abs/1203.3446.
[39] M. Maniatis, "The next-to-minimal supersymmetric extension of the standard model reviewed," *International Journal of Modern Physics A*, vol. 25, no. 18-19, pp. 3505–3602, 2010.
[40] U. Ellwanger, C. Hugonie, and A. M. Teixeira, "The next-to-minimal supersymmetric standard model," *Physics Reports*, vol. 496, no. 1-2, pp. 1–77, 2010.
[41] A. Djouadi, U. Ellwanger, and A. M. Teixeira, "Constrained next-to-minimal supersymmetric standard model," *Physical Review Letters*, vol. 101, no. 10, Article ID 101802, 2008.
[42] A. Djouadi, U. Ellwanger, and A. M. Teixeira, "Phenomenology of the constrained NMSSM," *Journal of High Energy Physics*, vol. 2009, no. 4, Article ID 031, 2009.
[43] E. Komatsu et al., "Seven-year wilkinson microwave anisotropy probe (WMAP *) observations: cosmological interpretation," *Astrophysical Journal*, vol. 192, no. 2, 2011.
[44] S. Chatrchyan et al., "Measurement of the neutrino velocity with the OPERA detector in the CNGS beam," *Physical Review Letters*, vol. 107, Article ID 221804, 2011.
[45] G. Aad et al., "Search for squarks and gluinos using final states with jets and missing transverse momentum with the Atlas detector in s=7 TeV proton-proton collisions," *Physics Letters B*, vol. 710, no. 1, pp. 67–85, 2012.
[46] CMS collaboration, "Search for supersymmetry with the razor variables at CMS," CMS-PAS-SUS-12-005.
[47] E. Aprile et al., "Dark matter results from 100 live days of XENON100 data," *Physical Review Letters*, vol. 107, no. 13, Article ID 131302, 2011.
[48] S. Schael et al., "ALEPH and DELPHI and L3 and OPAL Collaborations and LEP Working Group for Higgs Boson SearchesSearch for neutral MSSM Higgs bosons at LEP," *The European Physical Journal C*, vol. 47, no. 3, pp. 547–587, 2006.
[49] D. Das, U. Ellwanger, and A. M. Teixeira, "Modified signals for supersymmetry in the NMSSM with a singlino-like LSP," *Journal of High Energy Physics*, vol. 2012, no. 4, Article ID 067, 2012.
[50] ATLAS collaboration, "Search for supersymmetry in pp collisions at ps = 7 TeV in final states with missing transverse momentum and b-jets with the ATLAS detector," ATLAS-CONF-2012-003.
[51] D0 and CDF collaborations, "Search for scalar top and bottom quarks at the Tevatron," FERMILAB-CONF-09-108-E.
[52] G. W. Bennett et al., "Final report of the E821 muon anomalous magnetic moment measurement at BNL," *Physical Review D*, vol. 73, no. 7, Article ID 072003, 2006.

[53] Lepsusywg, Aleph, and Delphi, "L3 and OPAL experiments, notes LEPSUSYWG/04-01. 1 and 04-02. 1," http://lepsusy.web.cern.ch/lepsusy/.
[54] D. Collaboratio, V. M. Abazov, B. Abbott et al., "Search for the pair production of scalar top quarks in the acoplanar charm jet final state in $p\bar{p}$ collisions at $\sqrt{s} = 1.96$ TeV," *Physics Letters B*, vol. 645, no. 2-3, pp. 119–127, 2007.
[55] S. M. Wang CDF and D0 Collaborations, "Searches for squark and gluino production at the tevatron," *AIP Conference Proceedings*, vol. 1078, pp. 259–261, 2009.
[56] U. Ellwanger and C. Hugonie, "NMSPEC: a fortran code for the sparticle and Higgs masses in the NMSSM with GUT scale boundary conditions," *Computer Physics Communications*, vol. 177, no. 4, pp. 399–407, 2007.
[57] U. Ellwanger, J. F. Gunion, and C. Hugonie, "NMHDECAY: a fortran code for the Higgs masses, couplings and decay widths in the NMSSM," *Journal of High Energy Physics*, no. 2, pp. 1621–1661, 2005.
[58] U. Ellwanger and C. Hugonie, "NMHDECAY 2.1: an updated program for sparticle masses, Higgs masses, couplings and decay widths in the NMSSM," *Computer Physics Communications*, vol. 175, no. 4, pp. 290–303, 2006.
[59] G. Degrassi and P. Slavich, "On the radiative corrections to the neutral Higgs boson masses in the NMSSM," *Nuclear Physics B*, vol. 825, no. 1-2, pp. 119–150, 2010.
[60] S. Chatrchyan et al., "Search for neutral Higgs bosons decaying to tau pairs in pp collisions at sqrt(s)=7 TeV," *Physics Letters B*, vol. 713, no. 2, pp. 68–90, 2012.
[61] G. Bélanger, F. Boudjema, C. Hugonie, A. Pukhov, and A. Semenov, "Relic density of dark matter in the next-to-minimal supersymmetric standard model," *Journal of Cosmology and Astroparticle Physics*, no. 9, pp. 1–24, 2005.
[62] G. Bélanger, F. Boudjema, A. Pukhov, and A. Semenov, "micrOMEGAs 2.0: a program to calculate the relic density of dark matter in a generic model," *Computer Physics Communications*, vol. 176, no. 5, pp. 367–382, 2007.
[63] G. Bélanger, F. Boudjema, A. Pukhov, and A. Semenov, "Dark matter direct detection rate in a generic model with micrOMEGAs_2.2," *Computer Physics Communications*, vol. 180, no. 5, pp. 747–767, 2009.
[64] U. Ellwanger, "Enhanced di-photon higgs signal in the next-to-minimal supersymmetric standard model," *Physics Letters B*, vol. 698, no. 4, pp. 293–296, 2011.
[65] CDF and D0 collaborations, "Combined CDF and D0 Searches for Standard Model Higgs Boson Production," FERMILAB-CONF-12-065-E, CDF Note 10806, D0 Note 63032.
[66] R. Dermisek and J. F. Gunion, "A comparison of mixed-higgs scenarios in the NMSSM and the MSSM," *Physical Review D*, vol. 77, Article ID 015013, 2008.
[67] U. Ellwanger, "Higgs bosons in the Next-to-Minimal Supersymmetric Standard Model at the LHC," *The European Physical Journal C*, vol. 71, no. 10, p. 1782, 2011.
[68] U. Ellwanger, G. Espitalier-Noel, and C. Hugonie, "Naturalness and fine tuning in the NMSSM: implications of early LHC results," *JHEP*, vol. 2011, no. 09, p. 105, 2011.
[69] D. M. Ghilencea, H. M. Lee, and M. Park, "Tuning supersymmetric models at the LHC: a comparative analysis at two-loop level," *Journal of High Energy Physics*, vol. 2012, no. 7, article 046, 2012.